Heliyon 9 (2023) e17704

Contents lists available at ScienceDirect

Heliyon

journal homepage: www.cell.com/heliyon

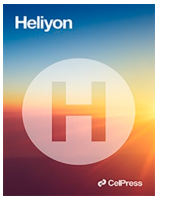

Fumaria officinalis-loaded chitosan nanoparticles dispersed in an alginate hydrogel promote diabetic wounds healing by upregulating VEGF, TGF-β, and b-FGF genes: A preclinical investigation

Xi Yang [a], Wenqian Mo [b], Yan Shi [a], Xiang Fang [a], Yujian Xu [a], Xiaoqing He [a], Yongqing Xu [a,*]

[a] Department of Orthopedics, 920 Hospital of Joint Logistic Support Force, Kunming, 650000, China
[b] Department of Pathology, Yunnan Cancer Hospital, The Third Affiliated Hospital of Kunming Medical University, Kunming, 650000, China

ARTICLE INFO

Keywords:
Fumaria officinalis extract
Chitosan nanoparticles
Alginate hydrogel
Diabetic wounds

ABSTRACT

Diabetic wounds may become chronic if left untreated. In the current study, a potential wound dressing was developed by incorporating fumaria officinalis extract-loaded chitosan nanoparticles (FOE-CHNPs) into calcium alginate hydrogel. The produced hydrogel was evaluated regarding its microarchitecture, cytotoxicity, cell migration activity, cytoprotective potential, porosity, in vitro anti-inflammatory activity, and drug release profile. Then, the healing function of FOE-CHNPs/calcium alginate hydrogel was compared with a marketed wound care product in a rat model of diabetic wound. In vitro study showed that the hydrogel system promoted skin cells viability and migration. In vivo wound healing assay showed that the animals treated with the FOE-CHNPs/calcium alginate hydrogel had comparable wound healing potential with the Granu-GEL® as the marketed wound care hydrogel. Gene expression studies showed that FOE-CHNPs/calcium alginate hydrogel upregulated the tissue expression levels of collagen type 1, collagen type 2, VEGF, b-FGF and TGF-B genes. This preclinical research, suggests potential use of FOE-loaded calcium alginate hydrogel system in treating diabetic wounds in the clinic.

1. Introduction

Current treatments for chronic wounds fail to restore skin's integrity, resulting in high rate of limb amputations, particularly in developing countries. Diabetic wounds arise due to intricate underlying factors. Prolonged high blood sugar levels harm tiny blood vessels, diminishing blood circulation and nutrient delivery. This, in turn, fosters an environment prone to infections due to compromised immunity and elevated glucose levels. Tissue strength is undermined as collagen production is affected. Furthermore, the presence of neuropathy, a prevalent diabetic condition, exacerbates the situation. Sensory neuropathy impairs sensation, rendering individuals unaware of injuries, while motor neuropathy disrupts biomechanics, intensifying pressure and friction on susceptible areas. Ultimately, diabetic wounds manifest as a consequence of impaired blood flow, compromised immunity, distorted collagen synthesis, and neuropathic alterations. A comprehensive understanding of these mechanisms is paramount for successful prevention

* Corresponding author.
E-mail address: dr_xyq774655@sina.com (Y. Xu).

https://doi.org/10.1016/j.heliyon.2023.e17704
Received 19 March 2023; Received in revised form 7 June 2023; Accepted 26 June 2023
Available online 29 June 2023

and management strategies [1–3]. Although significant progress has been made in developing bioactive wound dressing materials, the complex pathophysiology of the disease require a versatile approach for a successful wound healing [4–7]. In this context, various formulations of wound dressings such as nanofibers, hydrogels, membranes, wafers, sponges, and composites have been tested so far [8,9]. Among these options, hydrogel-based wound dressing materials offer overt advantages over other candidates such as a higher water content, ease of application in irregular shape wounds, cavity filling potential, high resemblance to skin's extracellular matrix, and easy functionalization [10–12]. These scaffolds are three-dimensional networks of polymers that can be fabricated using synthetic or natural polymers. However, hydrogels produced from natural polymers possess higher bioactivity and are generally cheaper [13]. In this framework, alginate-based hydrogels have been widely investigated for wound healing applications. This polymer is a natural polysaccharide that is obtained from brown algae [14,15]. Indeed, there are currently numerous alginate-based marketed wound care products. The main disadvantage of these wound dressings is that they do not possess sufficient bioactivity to alleviate oxidative stress and hyperactive inflammatory responses in the diabetic wounds tissues [16]. Therefore, recent studies have focused on incorporating drug delivery systems in the matrix of these hydrogels. Nanocomposite hydrogels play a crucial role in wound healing due to their unique properties. These materials combine the advantages of nanotechnology and hydrogel matrices, providing enhanced mechanical strength, controlled drug release, and biocompatibility. They promote cellular adhesion, proliferation, and tissue regeneration, making them promising for advanced wound care applications [1,2,17,18].

Bioactive agents with diverse pharmacological properties are available for this purpose. However, herbal medicine have broken new grounds in treating highly resistant diabetic wounds [19]. Fumaria officinalis is a medicinal plant that has been traditionally used for various diseases such as skin eczema, scabies, milk crust, and chronic inflammatory reactions [20,21]. The diverse biological functions of this plant such as its antiinflammatory, antibacterial, and antioxidative activities may be potentially beneficial to treat diabetic wounds [22]. The extract of fumaria officinalis (FOE) can be directly loaded into the hydrogel system. Despite being an straight forward strategy, this method may lead to a burst drug release as a result of hydrogel's swelling. This challenge can be addressed by incorporating a secondary drug carrier into the wound dressing material [23]. For example, chitosan nanoparticles (CHNPs) have been widely used in combination with hydrogel systems for wound healing applications. These drug carriers have a high encapsulation efficacy, sustained drug release ability, hemostatic activity, antibacterial properties, and an easy fabrication method [24]. In this research, FOE-loaded CHNPs were dispersed in the calcium alginate-based hydrogels to develop a potential treatment for diabetic wounds. The healing activity of this complex system was studied in a rat model of diabetic wound. This the first study developing a nanocomposite wound dressing system for delivering FOE for diabetic wound healing applications.

2. Methods and materials

2.1. Preparation of FOE-CHNPs and FOE-CHNPs/calcium alginate hydrogel

FOE-CHNPs were prepared using ionotropic gelation method as described previously [5]. Firstly, chitosan (low molecular weight, 85% deacetylation degree, Sigma Aldrich, USA) was dissolved in 1% v/v acetic acid (Glacial, Romil, UK) at 0.5 wt% concentration for 24 h and then filtered. Then, FOE (Hawaii Pharm, USA) was added to chitosan solution at 10% w/v and 20% w/v and stirred for 6 h. Tripolyphosphate pentasodium (Sigma Aldrich, USA) was dissolved in distilled water at 0.2% w/v and added to the chitosan/FOE solution at 20% v/v under strong stirring. Then, the resulting solution was centrifuged at 15,000 rpm for 45 min and the pellet was lyophilized for 48 h. Dry powder of nanoparticles were stored at 4 °C until use. Based on the weight ratio of FEO, FEO-loaded CHNPs were named FEO10%-CHNPs and FEO20%-CHNPs. Calcium alginate hydrogels were prepared by dissolving sodium alginate (medium viscosity, Sigma Aldrich, USA) in distilled water at 2 wt% for 24 h. Then, glycerol (Merck, Germany) was added to the sodium alginate solution at 40% w/w and mixed for 6 h at room temperature. Then, FEO-CHNPs were added to the sodium alginate solution at 15% w/w and stirred until homogenous dispersion. Finally, sodium alginate solution was crosslinked by dropwise addition of 2.5 wt% calcium chloride (Sigma Aldrich, USA) solution in distilled water at 20% v/v. The resulting hydrogel was lyophilized for in vitro characterizations.

2.2. Scanning electron microscopy (SEM)

The microstructure of lyophilized FEO-CHNPs and FOE-CHNPs/calcium alginate hydrogel was studied after coating them with gold for 250 s. After processing, SEM imaging was performed at 26 KV.

2.3. Encapsulation efficacy and drug release assay

The encapsulation efficacy of FEO into CHNPs and the release profile of FEO from and FOE-CHNPs/calcium alginate hydrogel was evaluated at 355 nm. After preparing the FEO-CHNPs, the solution was centrifuged at 15,000 rpm for 45 min and the amount of FEO in the supernatant was calculated. Following equation was used to calculate the encapsulation efficacy (EE):

$$\mathrm{EE}\ (\%) = \left(1 - \frac{\textit{Total amount of}\ \mathrm{FEO}\ \textit{in the supernatant}}{\textit{Initial amount of FEO}}\right) \times 100$$

For release assay, 150 mg of lyophilized FOE-CHNPs/calcium alginate hydrogel was immersed in 20 mL phosphate buffered saline (PBS) solution at 37 °C for 48 h. At different time points, the OD values of the release media samples was read at 355 nm and fir into the

standard curve of the FEO in PBS for the calculation of cumulative release profile.

2.4. Zeta potential and hydrodynamic particle size measurement

Hydrodynamic particle size and zeta potential of FOE-CHNPs and CHNPs were measured using photon correlation spectroscopy (PCS) (Zetasizer Nano-ZS-90, Malvern Instruments, Worcestershire, UK).

2.5. Water uptake capacity

Assessing the water uptake capacity of wound dressings is crucial as it determines their ability to maintain an optimal moisture environment, promoting wound healing. Adequate water absorption ensures proper hydration, exudate management, and prevention of tissue maceration, making it a vital characteristic for effective wound care. Lyophilized FOE-CHNPs/calcium alginate hydrogel were immersed in 20 mL PBS solution for 4 h. Then, scaffolds were removed and weighed. The dry and wet weight of each scaffold sample were used to calculate the water uptake capacity using a protocol as described previously [14].

2.6. Cell viability assay

L929 cells (murine fibroblast cell line, Pasture institute, Tehran, Iran) were seeded onto the lyophilized FOE-CHNPs/calcium alginate hydrogels at the density of 10,000 cells per scaffold and culture for 7 days using a previously-described method [5]. On days 2, 5, and 7 cell viability assay was carried out using an MTT assay kit (Abcam, USA).

2.7. Cytoprotection assay

L929 cells were seeded onto the lyophilized FOE-CHNPs/calcium alginate hydrogels at the density of 10,000 cells per scaffold and culture for 48 h. Then, 1% H_2O_2 v/v was added to the culture medium and incubated for 1 h. Cell viability was then assessed using an MTT assay kit (Abcam, USA). Cells cultured on the tissue culture plate without oxidative stress were used as the positive control group and cells cultured on the tissue culture plate with H_2O_2 were used as the negative control group.

2.8. Porosity measurement

The porosity of lyophilized FOE-CHNPs/calcium alginate hydrogels was evaluated using a liquid displacement method as described previously [25].

2.9. In vitro antiinflammatory assay

Lyophilized FOE-CHNPs/calcium alginate sponges were placed at 96-well plates and seeded with RAW 264.7 cells (monocyte/macrophage-like cells, Pasture institute, Tehran, Iran) at the density of 10,000 cells per each scaffold and cultured for 24 h. Then, the culture medium was supplemented with 1 μg/mL lipopolysaccharide (LPS) followed by incubation for 14 h. Then, the amount of IL-6 in the culture medium was measured using an ELIZA kit (Abcam, USA). Cells cultured on the tissue culture plate used as the control group.

2.10. In vitro wound healing assay

The effects of lyophilized sponges extract on the migration activity of L929 cells was evaluated. Briefly, 100 mg of each scaffold was immersed into 10 mL of DMEM culture medium (Gibco, USA) and kept for 48 h. Then, sponges were removed and the media was filtered and kept at 4 °C until use. Scratch test was carried out by seeding 1,250,000 L929 cells on a 24-well plate and culturing until a monolayer is formed. Then, the cellular monolayer was scratched using a 200 μl plastic pipette tip. The samples were then washed with PBS to discard the dead cells. Then, sponges extract in DMEM was supplemented with 0.5% FBS (Invitrogen, USA) and 1% 1% penicillin-streptomycin (Sigma Aldrich, USA). The resulting culture media was used for culturing the L929 cells for 48 h. On day 2, the wound size reduction was assessed using a light microscope and an image analysis software. Cells cultured without scaffolds extract used as the control group.

2.11. Animal studies

The animal experiments were performed in accordance with the U.K. Animals (Scientific Procedures) Act, 1986 and associated guidelines,EU Directive 2010/63/EU for animal experiments. Male Wistar rats (200–220 gr) were used for wound healing assay. The animals were injected with 55 mg/kg STZ for 7 days until their fasting blood sugar levels reached above 250 mg/dL. Fifteen diabetic rats were randomly divided into groups (three animals in each group): 1- Negative control group in which the wounded animals received no treatment, 2- FOE10%-CHNPs/calcium alginate hydrogel group, 3- FOE20%-CHNPs/calcium alginate hydrogels, 4- CHNPs/calcium alginate hydrogel group, and 5- GranuGEL® hydrogel wound dressing as the standard control. In each group, animals were anesthetized using ketamine-Xylazine cocktail. Then, the dorsal skin of the animals was shaved and cleaned with disinfectants.

The skin area was marked and an excisional wound (1.5 × 1.5 cm^2) was made using a surgical scissor. The hydrogels were applied on the wound site and a wet sterile gauze was used to cover the hydrogels. The treatment was repeated every two days until day 14th. On days 7 and 14, wound size reduction was evaluated by investigating the macroscopic appearance of the wounds and an image analysis software. After 14 days, the animals were sacrificed and the wound tissues were processed and sectioned for histopathological examinations. H&E and Masson's trichrome staining were used for measuring the thickness of epithelium and percentage of collagen deposition.

2.12. Gene expression analysis

Tissue expression levels of collagen type 1, collagen type 2, vascular endothelial growth factor (VEGF), basic fibroblast growth factor (b-FGF), transforming growth factor B (TGF-B), tumor necrosis factor-a, and IL-1β genes was evaluated after sacrificing the animals on day 14th. Briefly, tissue samples were minced into small pieces on ice and their RNA was isolated using an RNA isolation kit (Thermofisher. USA) and used for the synthesis of complementary DNA strands using an RNA reverse transcription kit (BioRad, USA). Then, predetermined volume of cDNA samples were mixed with Power SYBR® Green Master Mix (Thermofisher, USA). Relative gene expression of target genes was investigated using a protocol as described previously [26]. GAPDH gene was used as the house-keeping gene. Table 1 shows the primer sets for the target genes.

2.13. Statistical analysis

Date was analyzed using student's t-test and one-way ANOVA. Graph pad prism version 5 was used for plotting the graphs and data analysis.

3. Results

3.1. Microstructure studies

SEM images (Fig. 1) showed that FEO10%-CHNPs, FEO20%-CHNPs, and CHNPs had a spherical morphology with round shape. However, particles agglomerated in some spots. Particle size measurement showed that FEO10%-CHNPs, FEO20%-CHNPs had 252.80 ± 38.99 nm, 242.43 ± 35.86 nm, 254.90 ± 47.11 nm, respectively.

The SEM images of lyophilized hydrogels (Fig. 2) showed that FOE10%-CHNPs/calcium alginate, FOE20%-CHNPs/calcium alginate, and CHNPs/calcium alginate hydrogels were highly porous with a pore diameter around 50 μm.

3.2. Encapsulation efficacy and drug release assay

Encapsulation efficacy measurement showed that FEO was loaded into FEO10%-CHNPs with an efficacy around 52.55 ± 7.83%; while, encapsulation efficacy in FEO20%-CHNPs was 59.73 ± 5.93%. Release assay (Fig. 3) showed that at 48 h, cumulative drug release for FOE10%-CHNPs/calcium alginate and FOE20%-CHNPs/calcium alginate hydrogels was 61.58 ± 3.04% and 70.24 ± 4.43%, respectively.

3.3. Zeta potential and hydrodynamic particle size measurement assay

Results showed that FEO10%-CHNPs, FEO20%-CHNPs, and CHNPs had around +38.26 ± 9.01 mV, +34.97 ± 6.41 mV, and +39.98 ± 4.12 mV, respectively. Differences between groups were not statistically significant, p-value >0.05. The hydrodynamic particle size for FEO10%-CHNPs, FEO20%-CHNPs, and CHNPs was measured to be 454.08 ± 66.12 nm, 534.34 ± 37.08 nm, and 561.11 ± 68.65 nm, respectively.

3.4. Water uptake capacity measurement

Results showed that FOE10%-CHNPs/calcium alginate, and FOE20%-CHNPs/calcium alginate, and CHNPs/calcium alginate hydrogels had 334.19 ± 38.47%, 372.53 ± 33.96%, and 351.87 ± 25.78% water uptake capacity. Differences between groups were

Table 1
Primer sequences of target genes.

Target gene	Forward primer	Reverse primer
VEGF	TGCAGATTATGCGGATCAAACC	TGCATTCACATTTGTTGTGCTGTAG
b-FGF	CAATTCCCATGTGCTGTG	ACCTTGACCTCTCAGCC
Collagen type 2	GATTCCCTGGACCTAAAGGTGC	AGCCTCTCCATCTTTGCCAGCA
Collagen type 1	GATTCCCTGGACCTAAAGG	AGCCTCTCCATCTTTGCCAGC
TGF-β	ATTCCTGGCGTTACCTTGG	CCTGTATTCCGTCTCCTTGG
GAPDH	TCAACGGCACAGTCAAGG	TTCTGACTGGCAGTGATGG

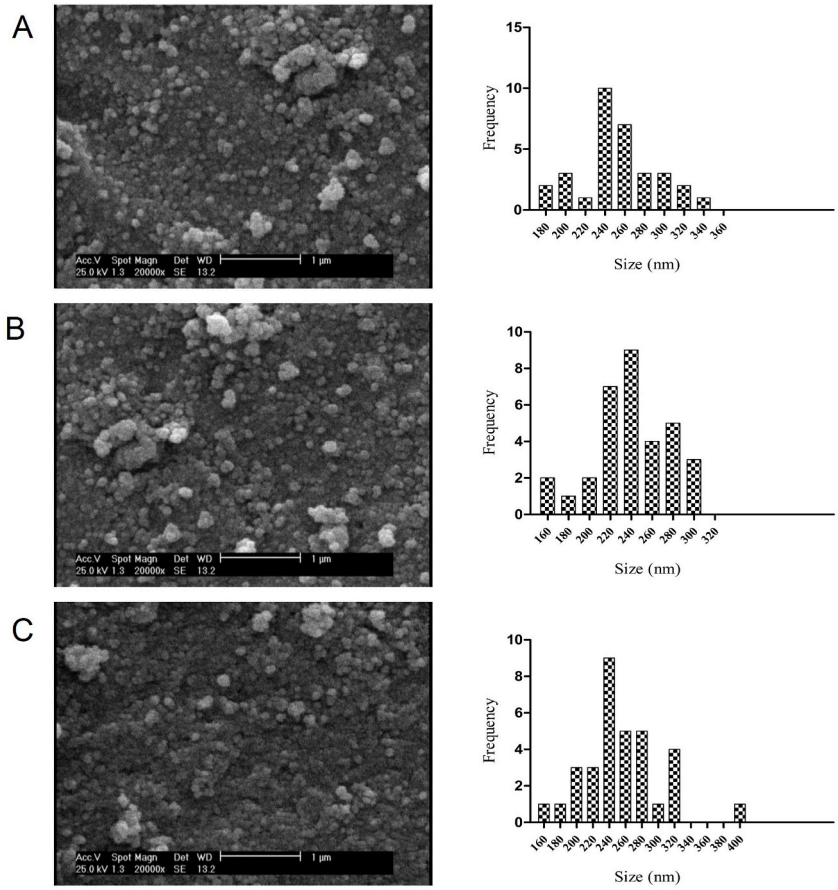

Fig. 1. Representative SEM images and particle size distribution of (A) FEO10%-CHNPs, (B) FEO20%-CHNPs, and (C) CHNPs.

not significant, p-value >0.05.

3.5. MTT assay under normal condition

Cell viability assay (Fig. 4) showed that on days 2 and 5; statistically, no significant difference was found between experimental groups, p-value >0.05, indicating that none of the scaffolds were toxic against L929 cells. On day 7, FOE20%-CHNPs/calcium alginate group had significantly higher cell viability than other groups, p-value <0.05.

3.6. Cytoprotection assay

Cytoprotection under assay (Fig. 5) in the presence of H2O2 showed that cells cultured on FOE10%-CHNPs/calcium alginate and FOE20%-CHNPs/calcium alginate hydrogels had significantly higher viability than the cells cultured on CHNPs/calcium alginate hydrogels, indicating that the presence of FEO in the wound dressing had protected cells against oxidative stress. Statistically, no significant difference was found between FOE10%-CHNPs/calcium alginate and FOE20%-CHNPs/calcium alginate groups, p-value >0.05.

3.7. Porosity measurement

Porosity measurement showed that FOE10%-CHNPs/calcium alginate, and FOE20%-CHNPs/calcium alginate, and CHNPs/calcium alginate hydrogels had 83.54 ± 7.23%, 80.23 ± 4.50%, and 78.25 ± 6.29% porosity. Differences between groups were not significant, p-value > 0.05.

3.8. In vitro antiinflammatory assay

Results (Fig. 6) showed that concentration of IL6 in FOE10%-CHNPs/calcium alginate and FOE20%-CHNPs/calcium alginate groups was significantly lower than CHNPs/calcium alginate and control groups, indicating that incorporation of FEO have imparted

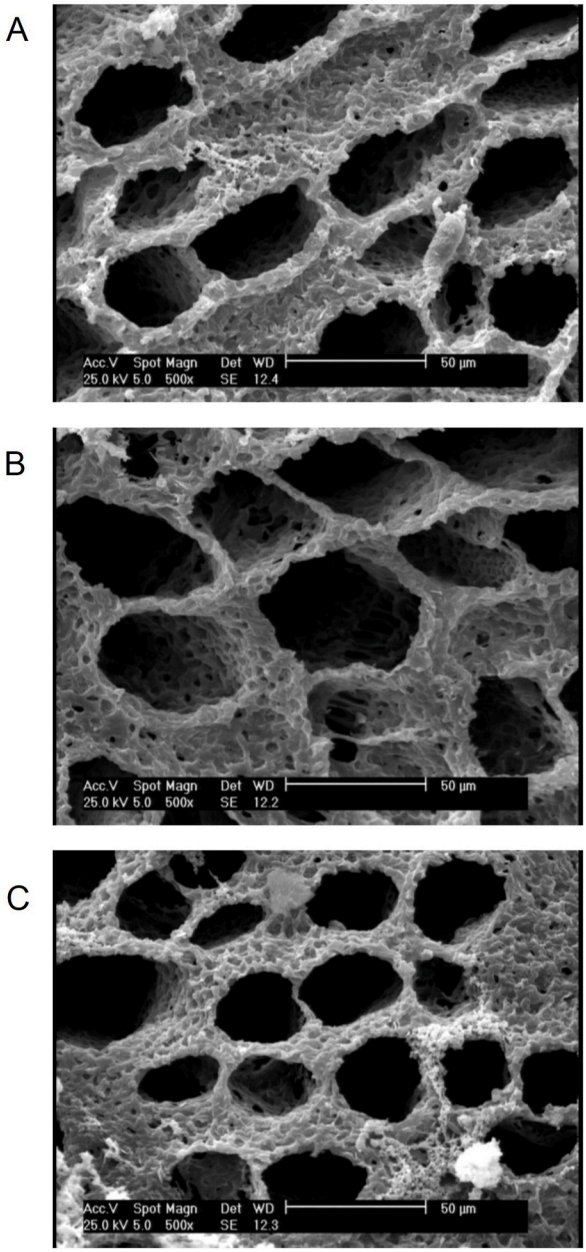

Fig. 2. Representative SEM images of (A) FOE10%-CHNPs/calcium alginate, (B) FOE20%-CHNPs/calcium alginate, and (C) CHNPs/calcium alginate sponges.

immunomodulatory activity to the dressings. Differences between FOE10%-CHNPs/calcium alginate and FOE20%-CHNPs/calcium alginate groups were not significant, p-value > 0.05.

3.9. In vitro wound healing

Wound closure assay (Fig. 7) showed that L929 cells cultured with the extract of FOE10%-CHNPs/calcium alginate and FOE20%-CHNPs/calcium alginate hydrogels had higher proliferation rate than control and CHNPs/calcium alginate hydrogel group that led to a significantly higher percentage of wound closure on day 2.

3.10. In vivo wound healing

Results of animal studies showed that GranuGEL® had the highest wound size reduction among experimental groups; however, its

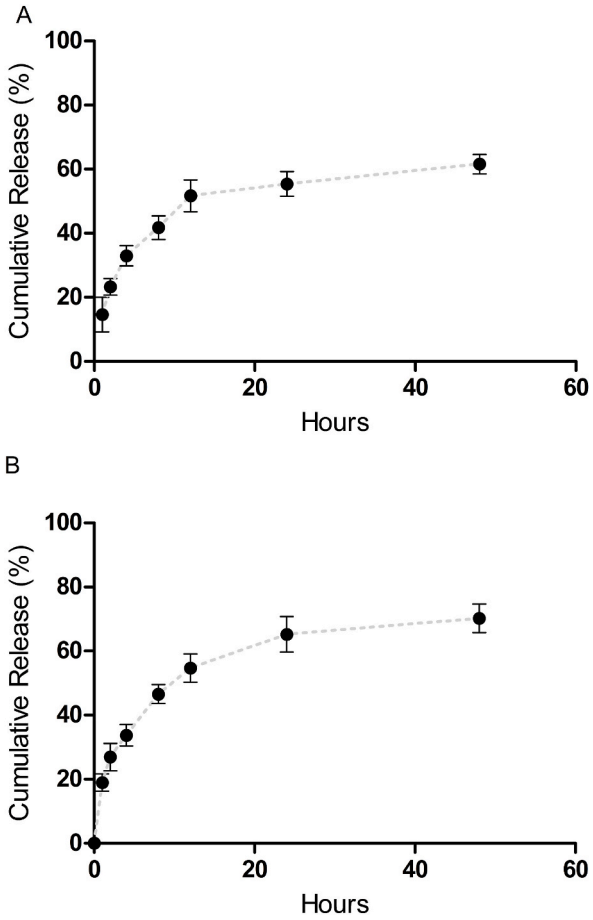

Fig. 3. Cumulative release profile of FEO from (A) FOE10%-CHNPs/calcium alginate and (B) FOE20%-CHNPs/calcium alginate hydrogels.

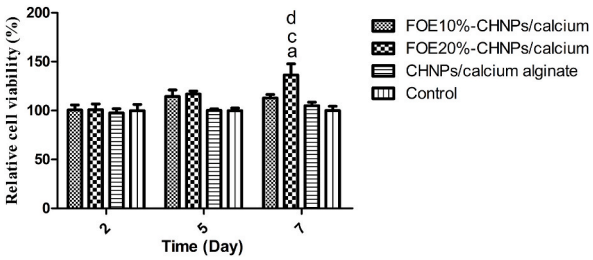

Fig. 4. Viability of L929 cells cultured on FOE10%-CHNPs/calcium alginate, FOE20%-CHNPs/calcium alginate, and CHNPs/calcium alginate hydrogels. Control group is the cells cultured on tissue culture plate, a shows p-value <0.05 relative to FOE10%-CHNPs/calcium alginate, c shows p-value <0.05 relative to CHNPs/calcium alginate group, and d shows p-value <0.05 relative to control group.

difference with FOE20%-CHNPs/calcium alginate was not significant, p-value >0.05 (Fig. 8). Wound closure for GranuGEL® group was 64.88 $\pm$ 3.76% and 97.77 $\pm$ 1.97% on day 7 and 14, respectively. FOE20%-CHNPs/calcium alginate and FOE10%-CHNPs/calcium alginate groups showed 93.06 $\pm$ 3.52% and 83.98 $\pm$ 5.08% wound size reduction on day 14 of post-wounding respectively. Histopathological studies (Fig. 9) showed that the wound site in the negative control group was poorly filled and was covered by a crusty scab. In addition, collagen deposition and epithelium formation occurred in a lower extent in this group compared with other groups. Infiltration of numerous inflammatory cells was also observed in this group. On the other hand, GranuGEL® and FOE20%-CHNPs/calcium alginate groups had a robust re-epithelialization and granulation tissue formation than other groups. Wound inflammation was significantly reduced and collagen fibers were more organized in these groups than other groups. Histomorphometric studies (Fig. 8) showed that FOE10%-CHNPs/calcium alginate and FOE20%-CHNPs/calcium alginate groups had significantly higher epithelium thickness and collagen deposition percentage than CHNPs/calcium alginate and negative control groups, p-value

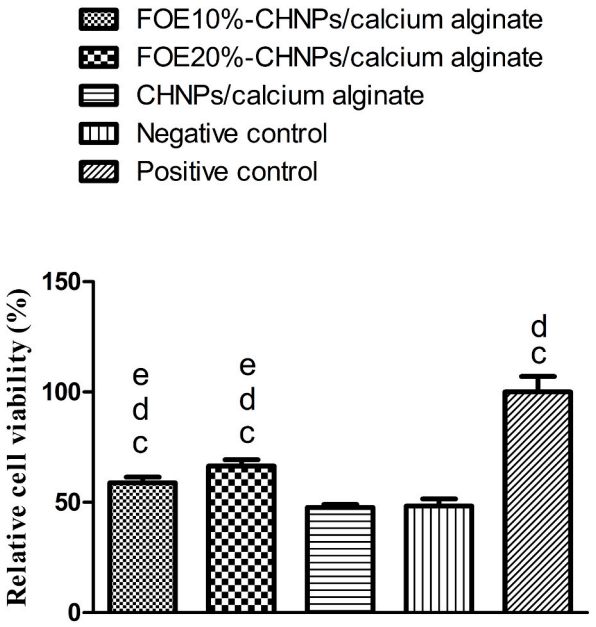

Fig. 5. Viability of L929 cells cultured on FOE10%-CHNPs/calcium alginate, FOE20%-CHNPs/calcium alginate, and CHNPs/calcium alginate hydrogels in the presence of 1% v/v H_2O_2. Negative control is the cells cultured with 1% v/v H_2O_2 without scaffolds and positive control group is the cells cultured with normal culture media, c shows p-value <0.05 relative to CHNPs/calcium alginate group, d shows p-value <0.05 relative to negative control group, and e shows p-value <0.05 relative to positive control group.

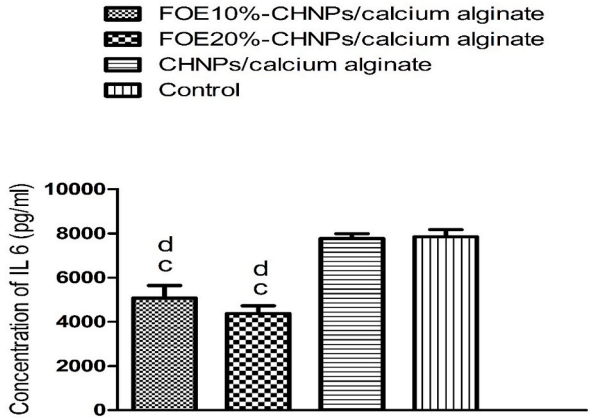

Fig. 6. Concentration of IL6 in the supernatant of RAW 264.7 cells cultured on FOE10%-CHNPs/calcium alginate, FOE20%-CHNPs/calcium alginate, and CHNPs/calcium alginate hydrogels, control group is the cells cultured without scaffolds, c shows p-value <0.05 relative to CHNPs/calcium alginate group and d shows p-value <0.05 relative to control group.

<0.05. Differences between FOE20%-CHNPs/calcium alginate and GranuGEL® groups were not statistically significant, p-value >0.05. Epithelium thickness for FOE10%-CHNPs/calcium alginate, FOE20%-CHNPs/calcium alginate, CHNPs/calcium alginate, Negative control, and GranuGEL® groups was 52.41 ± 4.25 μm, 53.79 ± 6.17 μm, 23.80 ± 3.26 μm, 23.66 ± 4.68 μm, 65.36 ± 4.77 μm, respectively. Collagen deposition for FOE10%-CHNPs/calcium alginate, FOE20%-CHNPs/calcium alginate, CHNPs/calcium alginate, Negative control, and GranuGEL® groups was measured to be 53.44 ± 3.67%, 65.48 ± 8.62%, 17.29 ± 3.89%, 13.39 ± 3.32%, 71.33 ± 6.97%, respectively.

3.11. Gene expression studies

Gene expression studies (Fig. 10) showed that GranuGEL® had significantly higher VEGF, collagen type II, and collagen type I genes expression levels than FOE10%-CHNPs/calcium alginate and FOE20%-CHNPs/calcium alginate groups, p-value <0.05. CHNPs/calcium alginate group had the lowest VEGF and collagen type II genes expression which was significantly lower than the expression

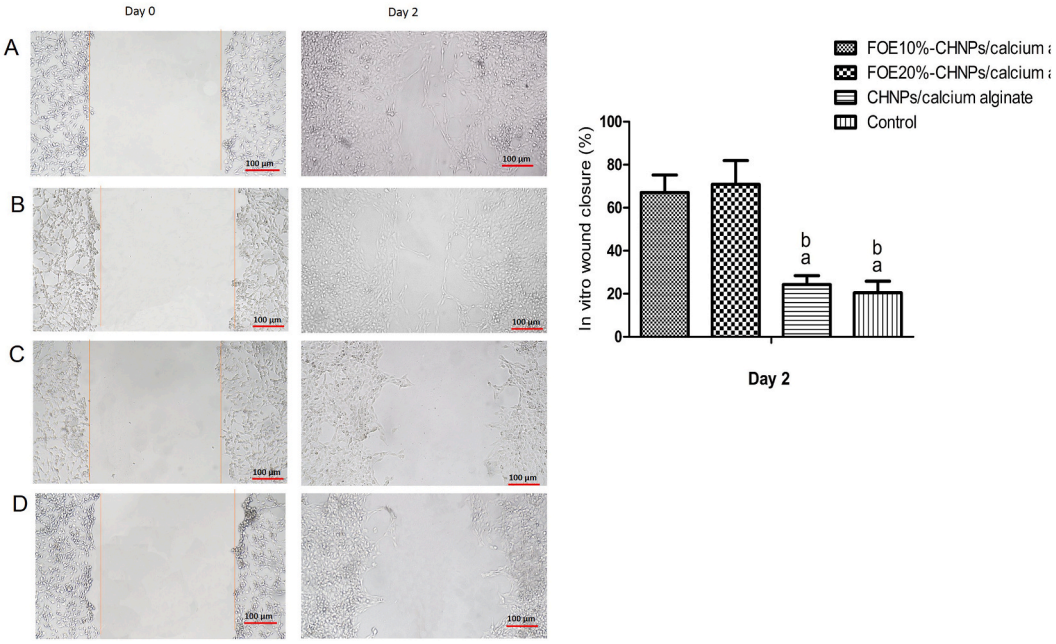

Fig. 7. In vitro wound closure with L929 cells cultured with the extract of (A) FOE10%-CHNPs/calcium alginate, (B) FOE20%-CHNPs/calcium alginate, and (C) CHNPs/calcium alginate hydrogels, (D) control group is the cells cultured without scaffolds, a shows p-value <0.05 relative to FOE10%-CHNPs/calcium alginate group and b shows p-value <0.05 relative to FOE20%-CHNPs/calcium alginate group.

level of these genes in FOE10%-CHNPs/calcium alginate and FOE20%-CHNPs/calcium alginate groups, p-value <0.05. Expression levels of b-FGF gene was significantly higher in GranuGEL® and FOE20%-CHNPs/calcium alginate groups than CHNPs/calcium alginate and FOE10%-CHNPs/calcium alginate groups, p-value <0.05. The expression levels of TGF-β gene was not significantly different among GranuGEL®, FOE20%-CHNPs/calcium alginate, and FOE10%-CHNPs/calcium alginate groups, p-value >0.05. However, this gene's expression was significantly lower in CHNPs/calcium alginate group than other groups, p-value <0.05. The expression levels of TNF-a and IL-1β genes were significantly lower in the wounds treated with FOE20%-CHNPs/calcium alginate and FOE10%-CHNPs/calcium alginate wound dressings than the wounds treated with CHNPs/calcium alginate, p-value <0.05. The differences between FOE20%-CHNPs/calcium alginate, FOE10%-CHNPs/calcium alginate, and GranuGEL® groups were not statistically significant, p-value >0.05.

4. Discussion

Drug-delivering wound dressings have gained significant momentum in diabetic wounds treatment. Here, a composite delivery vehicle for FOE was designed for sustained delivery of FOE into the diabetic wounds bed. The hydrogel compartment was intended to maintain a moist environment for wound healing; while, CHNPs provided the sustained release profile for FOE. Microstructure studies proved ultrasmall size of the FOE-CHNPs that may facilitate drug internalization into the skin cells. Indeed, CHNPs can improve drugs bioavailability by promoting drug diffusion through paracellular and intracellular pathways [27]. The porous microstructure of calcium alginate hydrogels may benefit wound healing, as these scaffolds act like an sponge and absorb wound exudates. The pores in the SEM images can be attributed to the evaporation of solvent-rich phase in the process of thermally induced phase separation [28]. The high encapsulation efficacy of FOE in FOE-CHNPs may be due to the hydrophobic or electrostatic interactions between FOE compounds and chitosan's matrix. However, this phenomenon was not elucidated in this research. FOE release from FOE10%-CHNPs/-calcium alginate and FOE20%-CHNPs/calcium alginate hydrogels faces two barriers; 1-the matrix of chitosan and 2-the matrix of calcium alginate. The Fick's law of diffusion may partly explain the release of FOE from the composite hydrogel [29]. However, the swelling of the hydrogel or gradual degradation of the polymeric matrix may also be involved in this process [30]. The positive zeta potential of the nanoparticles could be attributed to the presence of amine groups in the structure of chitosan [31]. Cell viability assays showed that FOE loading into the hydrogel system promoted L929 cells viability under normal and oxidative stress conditions. Indeed, various bioactive compounds in FOE such as alkaloids, flavonoids, saponins, and terpenoids may be responsible for its biological activities [32]. It could be that FOE has released from the hydrogel system and quenched ROS in the culture medium, resulting an increase in the cell viability in oxidative stress conditions. Indeed, the free radical scavenging activity of fumaria species has been well documented in previous studies. Abderrahim et al. showed that alkaloid fraction of FOE quenched DPPH, ABTS, and hypochlorous acid free radicals [33]. Paltinean et al. showed the potent antioxidant activity of six fumaria species including FOE [34]. Porosity of wound dressings is essential for gas exchange and preventing growth of anaerobic bacterial species [35]. However, lyophilized hydrogels have significantly higher percentage of porosity than un-lyophilized hydrogels. Hyperactivity of inflammatory responses retard the diabetic

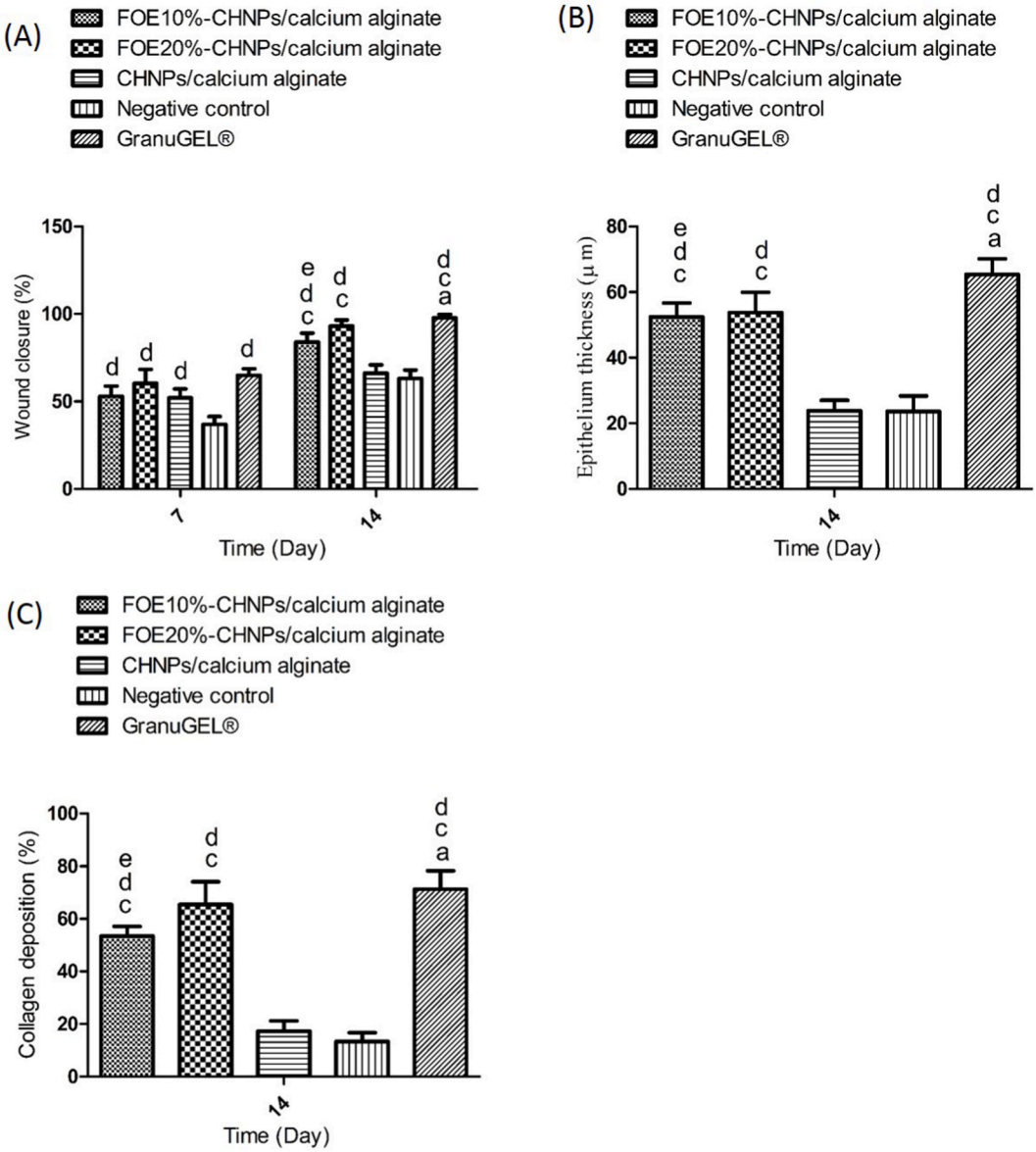

Fig. 8. Histograms comparing (A)wound closure percentage, (B) epithelium thickness, and (C) percentage of collagen deposition in wounds treated with different hydrogels, negative control group is the animals that received no treatment, a, b, c, d, and e show p-value <0.05 relative to FOE10%-CHNPs/calcium alginate, FOE20%-CHNPs/calcium alginate, CHNPs/calcium alginate, negative control, and GranuGEL® groups, respectively.

wound healing by damaging the tissues macromolecules. Therefore, immunomodulatory activity of wound dressings is of paramount importance in treating diabetic wounds [36]. In vitro anti-inflammatory assay showed that incorporation of FOE-CHNPs into calcium alginate hydrogels significantly decreased the concentration of IL-6 in the supernatant of macrophage cells, indicating that FOE has modulated inflammatory responses. Raafat et al. showed that two alkaloid fractions of FOE, namely Stylopine and Sanguinarine reduced the tissue expression level of pro-inflammatory cytokines including TNF-a and IL-6 [20]. Bioactive wound dressings promoting the migration activity of skin cells may promote higher wound closure. It has been shown that migration of keratocytes and fibroblast cells from the wound's edges plays a fundamental role in wound closure [37]. In vitro wound closure assay showed that fibroblast cells cultured with the extract of FOE10%-CHNPs/calcium alginate and FOE20%-CHNPs/calcium alginate had significantly higher migration activity, as evidenced by significantly higher in vitro wound closure percentage in these two groups compared with other groups. Little data is available in literature to explain this result and this part of our experiment needs further investigations. Wound healing assay showed that the wounds treated with FOE10%-CHNPs/calcium alginate and FOE20%-CHNPs/calcium alginate hydrogels had comparable healing activity with GranuGEL® as the standard control. It could be that FOE has released from the hydrogel system and protected the skin cells against oxidative stress through its antioxidative functions. This theory is in accordance

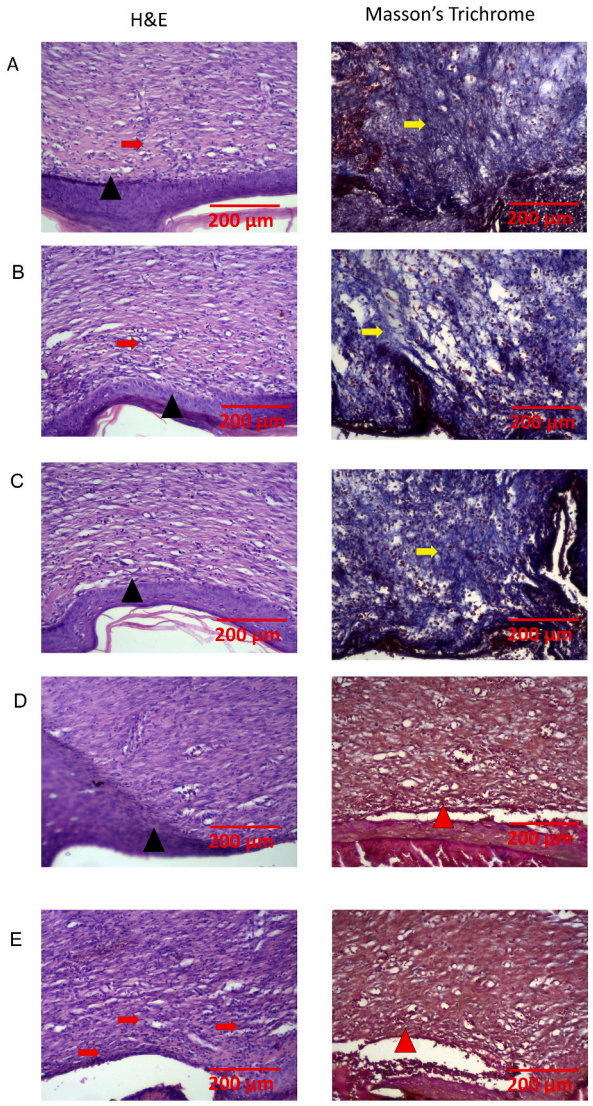

Fig. 9. Representative H&E and Masson's trichrome staining images of (A) GranuGEL, (B) FOE10%-CHNPs/calcium alginate, (C) FOE20%-CHNPs/calcium alginate, (D) CHNPs/calcium alginate, and (E) Negative control groups on day 14 after surgery, black triangles shows epithelial tissue, red triangles show unfilled defect site, red arrows shows inflammatory cells, and yellow arrows show collagen deposition. (For interpretation of the references to colour in this figure legend, the reader is referred to the Web version of this article.)

with the results of cytoprotection assay. Furthermore, FOE-CHNPs may have modulated inflammatory responses in diabetic wounds and augmented wound healing. Although in vitro experiments proved the immunomodulatory activity of FOE10%-CHNPs/calcium alginate and FOE20%-CHNPs/calcium alginate hydrogels, the tissue expression level of pro-inflammatory cytokines needs to be investigated. Collagen deposition and maturation is an essential process in wound healing [38]. As shown in histomorphometric studies the animals treated with FOE10%-CHNPs/calcium alginate and FOE20%-CHNPs/calcium alginate hydrogels had significantly higher percentage of wound closure than CHNPs/calcium alginate hydrogel and negative control groups. Furthermore, tissue expression levels of collagen type II and type I genes was significantly higher in FOE10%-CHNPs/calcium alginate and FOE20%-CHNPs/calcium alginate groups than other groups. Therefore, it can be assumed that FOE may have enhanced the tissue deposition of collagen and augmented wound healing. VEGF, TGF-β, and b-FGF genes are pro-healing genes that are activated in various stages of wound healing such as granulation tissue formation, tissue remodeling, and inflammation [39]. Upregulation of these genes via FOE10%-CHNPs/calcium alginate and FOE20%-CHNPs/calcium alginate hydrogels may partly explain the higher wound healing activity of these dressings than CHNPs/calcium alginate and negative control groups. The reduction of TNF-a and IL-1β genes via FOE loaded nanocomposite wound dressings implies that the extract has imparted anti-inflammatory potential to the dressings. Indeed, FOE possesses anti-inflammatory properties primarily attributed to its active compounds such as alkaloids and flavonoids. These bioactive constituents inhibit the production of pro-inflammatory mediators, including cytokines and prostaglandins.

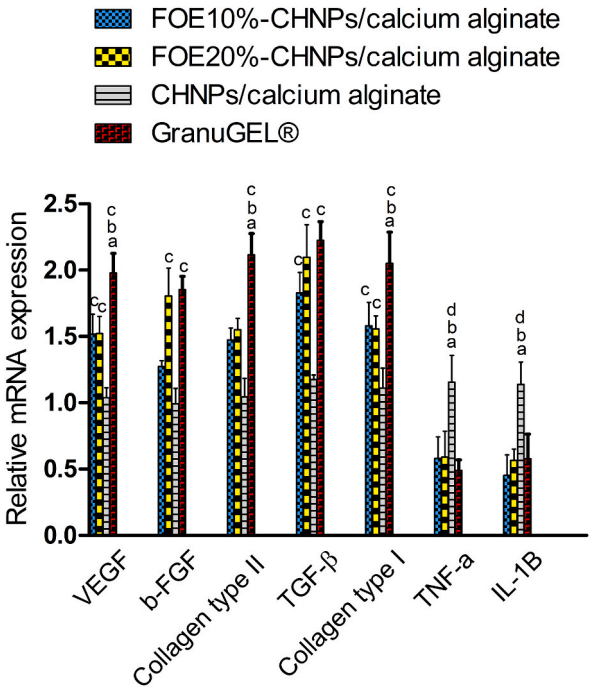

Fig. 10. Relative gene expression levels of different genes on day 14 after surgery, a, b, c, and d show p-value <0.05 relative to FOE10%-CHNPs/calcium alginate, FOE20%-CHNPs/calcium alginate, CHNPs/calcium alginate, and GranuGEL® groups, respectively.

Additionally, FOE may modulate the activity of inflammatory enzymes, such as cyclooxygenase and lipoxygenase. These mechanisms collectively contribute to its anti-inflammatory effects, potentially offering therapeutic benefits in various inflammatory conditions [40,41]. However, further experiments at protein expression levels and other genes are required to elucidate the exact mechanisms of the developed hydrogels' healing activity.

5. Conclusion

In this study, a composite delivery system was designed by incorporating FOE-loaded CHNPs into the matrix of calcium alginate hydrogels. In vitro experiments showed that FOE-loaded composite system were not toxic against L929 cells and promoted their migration activity. In vivo wound healing function of the developed delivery system was investigated in a rat model of diabetic wound. Wound closure, epithelial thickness, and collagen deposition were significantly greater in the animals treated with FOE-loaded hydrogels than other groups. Wound healing function of our developed system was comparable with GranuGEL® as the standard control. Gene expression studies showed that FOE-loaded hydrogels upregulated the tissue expression levels of VEGF, b-FGF, TGF-β, collagen type II, and collagen type I genes. This preclinical research, suggests potential use of FOE-loaded calcium alginate hydrogel system in treating diabetic wounds in the clinic.

Author contribution statement

Xi Yang: Conceived and designed the experiments; Performed the experiments; Contributed reagents, materials, analysis tools or data; Wrote the paper.

Yongqing Xu: Conceived and designed the experiments.

Wenqian Mo, Yan Shi, Xiang Fang: Performed the experiments; Analyzed and interpreted the data; Contributed reagents, materials, analysis tools or data; Wrote the paper.

Yujian Xu, Xiaoqing He Performed the experiments; Contributed reagents, materials, analysis tools or data; Wrote the paper.

Data availability statement

Data will be made available on request.

Declaration of competing interest

The authors declare that they have no known competing financial interests or personal relationships that could have appeared to

influence the work reported in this paper.

Acknowledgments

This research was supported by Yunnan Provincial Science and Technology Plan Project, Kunming Medical University Applied Basic Research Joint Project (No. 202201AY70001-292).

References

[1] X. Xu, Y. Zeng, Z. Chen, Y. Yu, H. Wang, X. Lu, J. Zhao, S. Wang, Chitosan-based multifunctional hydrogel for sequential wound inflammation elimination, infection inhibition, and wound healing, Int. J. Biol. Macromol. 235 (2023), 123847.
[2] Z. Chen, J. Yao, J. Zhao, S. Wang, Injectable wound dressing based on carboxymethyl chitosan triple-network hydrogel for effective wound antibacterial and hemostasis, Int. J. Biol. Macromol. 225 (2023) 1235–1245.
[3] J.L. Burgess, W.A. Wyant, B. Abdo Abujamra, R.S. Kirsner, I. Jozic, Diabetic wound-healing science, Medicina 57 (2021) 1072.
[4] H. Samadian, S. Zamiri, A. Ehterami, S. Farzamfar, A. Vaez, H. Khastar, M. Alam, A. Ai, H. Derakhshankhah, Z. Allahyari, Electrospun cellulose acetate/gelatin nanofibrous wound dressing containing berberine for diabetic foot ulcer healing: in vitro and in vivo studies, Sci. Rep. 10 (2020) 1–12.
[5] A. Ehterami, M. Salehi, S. Farzamfar, A. Vaez, H. Samadian, H. Sahrapeyma, M. Mirzaii, S. Ghorbani, A. Goodarzi, In vitro and in vivo study of pcl/coll wound dressing loaded with insulin-chitosan nanoparticles on cutaneous wound healing in rats model, Int. J. Biol. Macromol. 117 (2018) 601–609.
[6] S. Shafei, M. Khanmohammadi, R. Heidari, H. Ghanbari, V. Taghdiri Nooshabadi, S. Farzamfar, M. Akbariqomi, N.S. Sanikhani, M. Absalan, G. Tavoosidana, Exosome loaded alginate hydrogel promotes tissue regeneration in full-thickness skin wounds: an in vivo study, J. Biomed. Mater. Res. 108 (2020) 545–556.
[7] S. Cheng, H. Wang, X. Pan, C. Zhang, K. Zhang, Z. Chen, W. Dong, A. Xie, X. Qi, Dendritic hydrogels with robust inherent antibacterial properties for promoting bacteria-infected wound healing, ACS Appl. Mater. Interfaces 14 (2022) 11144–11155.
[8] M. Salehi, K. Shahporzadeh, A. Ehterami, H. Yeganehfard, H. Ziaei, M.M. Azizi, S. Farzamfar, A. Tahersoltani, A. Goodarzi, J. Ai, Electrospun poly (ε-caprolactone)/gelatin nanofibrous mat containing selenium as a potential wound dressing material: in vitro and in vivo study, Fibers Polym. 21 (2020) 1713–1721.
[9] S. Farzamfar, M. Naseri-Nosar, H. Samadian, S. Mahakizadeh, R. Tajerian, M. Rahmati, A. Vaez, M. Salehi, Taurine-loaded poly (ε-caprolactone)/gelatin electrospun mat as a potential wound dressing material: in vitro and in vivo evaluation, J. Bioact. Compat Polym. 33 (2018) 282–294.
[10] Y. Liang, B. Chen, M. Li, J. He, Z. Yin, B. Guo, Injectable antimicrobial conductive hydrogels for wound disinfection and infectious wound healing, Biomacromolecules 21 (2020) 1841–1852.
[11] M. Zhang, Y. Huang, W. Pan, X. Tong, Q. Zeng, T. Su, X. Qi, J. Shen, Polydopamine-incorporated dextran hydrogel drug carrier with tailorable structure for wound healing, Carbohydr. Polym. 253 (2021), 117213.
[12] Y. Xiang, X. Qi, E. Cai, C. Zhang, J. Wang, Y. Lan, H. Deng, J. Shen, R. Hu, Highly efficient bacteria-infected diabetic wound healing employing a melanin-reinforced biopolymer hydrogel, Chem. Eng. J. 460 (2023), 141852.
[13] M. Kharaziha, A. Baidya, N. Annabi, Rational design of immunomodulatory hydrogels for chronic wound healing, Adv. Mater. 33 (2021), 2100176.
[14] A. Ehterami, M. Salehi, S. Farzamfar, H. Samadian, A. Vaez, S. Ghorbani, J. Ai, H. Sahrapeyma, Chitosan/alginate hydrogels containing alpha-tocopherol for wound healing in rat model, J. Drug Deliv. Sci. Technol. 51 (2019) 204–213.
[15] A. Ehterami, M. Salehi, S. Farzamfar, H. Samadian, A. Vaez, H. Sahrapeyma, S. Ghorbani, A promising wound dressing based on alginate hydrogels containing vitamin d3 cross-linked by calcium carbonate/d-glucono-δ-lactone, Biomed. Eng. Lett. 10 (2020) 309–319.
[16] C.M. Cleetus, F.A. Primo, G. Fregoso, N.L. Raveendran, J.C. Noveron, C.T. Spencer, C.V. Ramana, B. Joddar, Alginate hydrogels with embedded zno nanoparticles for wound healing therapy, Int. J. Nanomed. 15 (2020) 5097.
[17] T. Wang, W. Yi, Y. Zhang, H. Wu, H. Fan, J. Zhao, S. Wang, Sodium alginate hydrogel containing platelet-rich plasma for wound healing, Colloids Surf. B Biointerfaces 222 (2023), 113096.
[18] Y. Ouyang, J. Zhao, S. Wang, Multifunctional hydrogels based on chitosan, hyaluronic acid and other biological macromolecules for the treatment of inflammatory bowel disease: a review, Int. J. Biol. Macromol. (2022).
[19] T. Maver, U. Maver, K. Stana Kleinschek, D.M. Smrke, S. Kreft, A review of herbal medicines in wound healing, Int. J. Dermatol. 54 (2015) 740–751.
[20] K.M. Raafat, S.A. El-Zahaby, Niosomes of active fumaria officinalis phytochemicals: antidiabetic, antineuropathic, anti-inflammatory, and possible mechanisms of action, Chin. Med. 15 (2020) 1–22.
[21] C. Li, Y. Zhang, M. Li, H. Zhang, Z. Zhu, Y. Xue, Fumaria officinalis-assisted synthesis of manganese nanoparticles as an anti-human gastric cancer agent, Arab. J. Chem. 14 (2021), 103309.
[22] H. Edziri, M. Guerrab, R. Anthonissen, M. Mastouri, L. Verschaeve, Phytochemical screening, antioxidant, anticoagulant and in vitro toxic and genotoxic properties of aerial parts extracts of fumaria officinalis l. Growing in Tunisia, South Afr. J. Bot. 130 (2020) 268–273.
[23] S. Saghazadeh, C. Rinoldi, M. Schot, S.S. Kashaf, F. Sharifi, E. Jalilian, K. Nuutila, G. Giatsidis, P. Mostafalu, H. Derakhshandeh, Drug delivery systems and materials for wound healing applications, Adv. Drug Deliv. Rev. 127 (2018) 138–166.
[24] N. Aibani, R. Rai, P. Patel, G. Cuddihy, E.K. Wasan, Chitosan nanoparticles at the biological interface: implications for drug delivery, Pharmaceutics 13 (2021) 1686.
[25] M. Salehi, M. Naseri-Nosar, S. Ebrahimi-Barough, M. Nourani, A. Khojasteh, A.A. Hamidieh, A. Amani, S. Farzamfar, J. Ai, Sciatic nerve regeneration by transplantation of schwann cells via erythropoietin controlled-releasing polylactic acid/multiwalled carbon nanotubes/gelatin nanofibrils neural guidance conduit, J. Biomed. Mater. Res. B Appl. Biomater. 106 (2018) 1463–1476.
[26] M. Rezaii, S. Oryan, A. Javeri, Curcumin nanoparticles incorporated collagen-chitosan scaffold promotes cutaneous wound healing through regulation of tgf-β1/smad7 gene expression, Mater. Sci. Eng. C 98 (2019) 347–357.
[27] S. Shim, H.S. Yoo, The application of mucoadhesive chitosan nanoparticles in nasal drug delivery, Mar. Drugs 18 (2020) 605.
[28] H. Samadian, S. Farzamfar, A. Vaez, A. Ehterami, A. Bit, M. Alam, A. Goodarzi, G. Darya, M. Salehi, A tailored polylactic acid/polycaprolactone biodegradable and bioactive 3d porous scaffold containing gelatin nanofibers and taurine for bone regeneration, Sci. Rep. 10 (2020) 1–12.
[29] I.R. Calori, G. Braga, P. d C.C. de Jesus, H. Bi, A.C. Tedesco, Polymer scaffolds as drug delivery systems, Eur. Polym. J. 129 (2020), 109621.
[30] R. Ferracini, I. Martínez Herreros, A. Russo, T. Casalini, F. Rossi, G. Perale, Scaffolds as structural tools for bone-targeted drug delivery, Pharmaceutics 10 (2018) 122.
[31] A.S. Tzeyung, S. Md, S.K. Bhattamisra, T. Madheswaran, N.A. Alhakamy, H.M. Aldawsari, A.K. Radhakrishnan, Fabrication, optimization, and evaluation of rotigotine-loaded chitosan nanoparticles for nose-to-brain delivery, Pharmaceutics 11 (2019) 26.
[32] R. Zhang, Q. Guo, E.J. Kennelly, C. Long, X. Chai, Diverse alkaloids and biological activities of fumaria (papaveraceae): an ethnomedicinal group, Fitoterapia 146 (2020), 104697.
[33] S. Khamtache-Abderrahim, S. Yahiaoui, A. Otmani, M. Bachir-Bey, Optimization of Phenolic Compound Recovery and Antioxidant Activity from Fumaria Officinalis L. Using Response Surface Methodology, vol. 45, The Annals of the University Dunarea de Jos of Galati. Fascicle VI-Food Technology, 2021, pp. 117–133.
[34] R. Păltinean, A. Mocan, L. Vlase, A.-M. Gheldiu, G. Crișan, I. Ielciu, O. Voștinaru, O. Crișan, Evaluation of polyphenolic content, antioxidant and diuretic activities of six fumaria species, Molecules 22 (2017) 639.
[35] R. Dong, B. Guo, Smart wound dressings for wound healing, Nano Today 41 (2021), 101290.
[36] S.K. Shukla, A.K. Sharma, V. Gupta, M. Yashavarddhan, Pharmacological control of inflammation in wound healing, J. Tissue Viability 28 (2019) 218–222.

[37] M. Ottosson, A. Jakobsson, F. Johansson, Accelerated wound closure-differently organized nanofibers affect cell migration and hence the closure of artificial wounds in a cell based in vitro model, PLoS One 12 (2017), e0169419.
[38] R. Zinder, R. Cooley, L.G. Vlad, J.A. Molnar, Vitamin a and wound healing, Nutr. Clin. Pract. 34 (2019) 839–849.
[39] S. Yamakawa, K. Hayashida, Advances in surgical applications of growth factors for wound healing, Burns Trauma 7 (2019).
[40] K.M. Raafat, S.A. El-Zahaby, Niosomes of active fumaria officinalis phytochemicals: antidiabetic, antineuropathic, anti-inflammatory, and possible mechanisms of action, Chin. Med. 15 (2020) 1–22.
[41] F. Iraji, B.S. Makhmalzadeh, M. Abedini, A. Aghaei, A. Siahposh, Effect of herbal cream containing fumaria officinalis and silymarin for treatment of eczema: a randomized double-blind controlled clinical trial, Avicenna J. Phytomed. 12 (2022) 155.